

Manifestation of impurity induced $s_{\pm} \implies s_{++}$ transition: multiband model for dynamical response functions

D.V. Efremov

E-mail: efremov@fkf.mpg.de

Max-Planck-Institut für Festkörperforschung, D-70569 Stuttgart, Germany, IFW
Dresden, Helmholtzstrasse 20, D-01069 Dresden, Germany

A.A. Golubov

Faculty of Science and Technology and MESA+ Institute of Nanotechnology,
University of Twente, 7500 AE Enschede, The Netherlands

O.V. Dolgov

Max-Planck-Institut für Festkörperforschung, D-70569 Stuttgart, Germany

Submitted to: *New J. Phys.*

Abstract. We investigate effects of disorder on the density of states, the single particle response function and optical conductivity in multiband superconductors with s_{\pm} symmetry of the order parameter, where $s_{\pm} \rightarrow s_{++}$ transition may take place. In the vicinity of the transition the superconductive gapless regime is realized. It manifests itself in anomalies in the above mentioned properties. As a result, intrinsically phase-insensitive experimental methods like ARPES, tunneling and terahertz spectroscopy may be used for revealing of information about the underlying order parameter symmetry.

PACS numbers: 71.10.Ay, 75.30.Cr, 74.25.Ha, 74.25.Jb

1. Introduction

The discovery of iron-based superconductors [1] (FeSC) put forward experimental and theoretical efforts to understand the reason for rather high critical temperatures and symmetry of superconducting order parameters in these compounds. These studies yielded a comprehensive experimental description of the electronic Fermi surface structure, which includes multiple Fermi surface sheets in a good agreement with density functional calculations [2]. The Fermi surface of the moderate doped FeSC is given by two small hole pockets around $\Gamma = (0,0)$ point and two electron pockets around $M = (\pi, \pi)$ point in the folded zone. This band structure suggests strong antiferromagnetic fluctuations, which may be a mechanism for electron pairing. In this case, the natural order parameter for most of the FeSC is so called s_{\pm} state, described by the nodeless order parameter with different signs for electron and hole-like pockets.

This model agrees well with the experimentally found for most of the moderately doped Fe-based superconductors nodeless character of the order parameter [3, 4, 5, 6]. However a question, whether the order parameter changes its sign by changeover from electron-like to hole-like pockets, is still under discussion. Moreover, relative robustness of the superconductors against nonmagnetic impurities led to a suggestion that a more conventional two-band order parameter a uniform sign change (s_{++}) is realized in these systems [7].

In our previous paper [8] it was demonstrated that not only superconductors with s_{++} order parameter but also s_{\pm} may be robust against nonmagnetic impurities. Therefore the robustness against nonmagnetic impurities can not be considered as a strong argument against s_{\pm} order parameter. Moreover, it was shown, that there are two types of s_{\pm} -superconductors with respect to disorder [8]. In the first one T_c goes down as disorder is increased, until it vanishes at a critical value of the scattering rate. This behavior is similar to the famous case of Abrikosov-Gor'kov magnetic impurities. It is widely discussed in the literature. In the second type of s_{\pm} superconductors T_c tends to a finite value as disorder is increased [9, 10]; at the same time the gap functions for the electron-like and hole-like Fermi surfaces acquire the same signs, i.e. the transition occurs from s_{\pm} to s_{++} .

In the present paper we discuss how the disorder induced transition $s_{\pm} \rightarrow s_{++}$ can display itself in single particle properties and optical conductivity. It is shown that disorder dependence of these characteristics at the transition point is strongly nonmonotonic function of the impurity scattering rate and can be easily seen in tunneling spectroscopy, ARPES and optics. Therefore systematic study of disorder effects by means formally phase insensitive techniques, mentioned above, may provide information about the sign of the underlying order parameter in the clean limit.

The paper is organized as follows. In the section II we discuss the approximation used for the calculations. The section III is devoted to single particle properties. We discuss how the transition $s_{\pm} \rightarrow s_{++}$ manifests itself in ARPES and tunneling spectroscopy. In the section III we calculate the two-particle response function and

discuss peculiarities which can be seen in optical conductivity in the vicinity of the transition point. The article is concluded with discussions.

2. The formalism

For the calculations we employ the standard approach of quasiclassical (ξ - integrated) Green functions in Nambu and band space [11]:

$$\hat{\mathbf{g}}(\omega) = \begin{pmatrix} \mathbf{g}_a & 0 \\ 0 & \mathbf{g}_b \end{pmatrix}, \quad (1)$$

with band quasiclassical Green functions

$$\mathbf{g}_{\alpha}(\omega) = -i\pi N_{\alpha} \frac{\tilde{\omega}_{\alpha}\hat{\tau}_0 + \tilde{\phi}_{\alpha}\hat{\tau}_1}{\sqrt{\tilde{\omega}_{\alpha}^2 - \tilde{\phi}_{\alpha}^2}}, \quad (2)$$

where the $\hat{\tau}_i$ denote Pauli matrices in Nambu space and N_{α} is the density of states on the Fermi level in the band $\alpha = a, b$ (for the sake of simplicity the two band model is considered).

The function $\hat{\mathbf{g}}_{\alpha}$ is related to the full Green function

$$\hat{\mathbf{G}}_{\alpha}(\mathbf{k}, \omega_n) = \frac{\tilde{\omega}_{\alpha}\hat{\tau}_0 + \xi_{\alpha}(\mathbf{k})\hat{\tau}_3 + \tilde{\phi}_{\alpha}\hat{\tau}_1}{\tilde{\omega}_{\alpha}^2 - \xi_{\alpha}^2(\mathbf{k}) - \tilde{\phi}_{\alpha}^2} \quad (3)$$

by the standard procedure of ξ -integration $\hat{\mathbf{g}}_{\alpha}(\omega) = N_{\alpha} \int d\xi_{\alpha}(\mathbf{k}) \hat{\mathbf{G}}_{\alpha}(\mathbf{k}, \omega)$.

The quasiclassical Green functions are obtained by numerical solution of the Eliashberg equations:

$$\tilde{\omega}_{\alpha}(\omega) - \omega = \sum_{\beta=a,b} \left\{ \int_{-\infty}^{\infty} dz K_{\alpha\beta}^{\omega}(z, \omega) \operatorname{Re} \frac{\tilde{\omega}_{\beta}(z)}{\sqrt{\tilde{\omega}_{\beta}^2(z) - \tilde{\phi}_{\beta}^2(z)}} + i\Gamma_{\alpha\beta}(\omega) \frac{\tilde{\omega}_{\beta}(\omega)}{\sqrt{\tilde{\omega}_{\beta}^2(\omega) - \tilde{\phi}_{\beta}^2(\omega)}} \right\}, \quad (4)$$

$$\tilde{\phi}_{\alpha}(\omega) = \sum_{\beta=a,b} \left\{ \int_{-\infty}^{\infty} dz K_{\alpha\beta}^{\phi}(z, \omega) \operatorname{Re} \frac{\tilde{\phi}_{\beta}(z)}{\sqrt{\tilde{\omega}_{\beta}^2(z) - \tilde{\phi}_{\beta}^2(z)}} + i\Gamma_{\alpha\beta}(\omega) \frac{\tilde{\phi}_{\beta}(\omega)}{\sqrt{\tilde{\omega}_{\beta}^2(\omega) - \tilde{\phi}_{\beta}^2(\omega)}} \right\}, \quad (5)$$

where the kernels $K_{\alpha\beta}^{\tilde{\phi}, \tilde{\omega}}(z, \omega)$ have the standard form:

$$K_{\alpha\beta}^{\tilde{\phi}, \tilde{\omega}}(z, \omega) = \int_{-\infty}^{\infty} d\Omega \frac{\lambda_{\alpha\beta}^{\tilde{\phi}, \tilde{\omega}} B(\Omega)}{2} \times \left[\frac{\tanh \frac{z}{2T} + \coth \frac{\Omega}{2T}}{z + \Omega - \omega - i\delta} \right]. \quad (6)$$

For simplicity we use the same normalized spectral function of electron-boson interaction $B(\Omega)$ for all the channels, which is presented in inset Fig. 2. The maximum of the spectra is $\Omega_{sf} = 18$ meV [6]. The matrix elements $\lambda_{\alpha\beta}^{\tilde{\phi}}$ are positive for attractive interactions and negative for repulsive ones. The symmetry of the order parameter in the clean case is determined solely by the off-diagonal matrix elements. The case $\operatorname{sign}\lambda_{ab}^{\tilde{\phi}} = \operatorname{sign}\lambda_{ba}^{\tilde{\phi}} > 0$ corresponds to s_{++} superconductivity and $\operatorname{sign}\lambda_{ab}^{\tilde{\phi}} = \operatorname{sign}\lambda_{ba}^{\tilde{\phi}} < 0$ to s_{\pm} . The matrix elements $\lambda_{\alpha\beta}^{\tilde{\omega}}$ have to be positive and are chosen $\lambda_{\alpha\beta}^{\tilde{\omega}} = |\lambda_{\alpha\beta}^{\tilde{\phi}}|$. For

further calculations we use the same matrix $\lambda_{aa}^{\tilde{\phi}} = 3$, $\lambda_{bb}^{\tilde{\phi}} = 0.5$, $\lambda_{ab}^{\tilde{\phi}} = -0.2$, $\lambda_{ba}^{\tilde{\phi}} = -0.1$ for s_{\pm} -case and $\lambda_{aa}^{\tilde{\phi}} = 3$, $\lambda_{bb}^{\tilde{\phi}} = 0.5$, $\lambda_{ab}^{\tilde{\phi}} = 0.2$, $\lambda_{ba}^{\tilde{\phi}} = 0.1$ for s_{++} -case. The correspondent ratio of the densities of states is $N_a/N_b = 0.5$ (see [8]).

The second terms in the right side of the Eqs.(4-5) reflect scattering on impurities. In the general case $\Gamma_{\alpha\beta}(\omega)$ can be written in the following form:

$$\Gamma_{\alpha\beta}(\omega) = \gamma_{\alpha\beta}^N I(\omega), \quad (7)$$

where the $\gamma_{\alpha\beta}^N$ are inter- and intra-band impurity scattering rates in the normal state. The dynamical part $I(\omega) = 1$ in Born approximation (see Appendix). Beyond the Born approximation it reads:

$$I(\omega) = \frac{1}{1 - 2\zeta C_{ab}(\omega)}, \quad (8)$$

where $C_{ab}(\omega)$ is the *coherence factor*:

$$C_{ab}(\omega) = 1 - \frac{\tilde{\omega}_a \tilde{\omega}_b - \tilde{\phi}_a \tilde{\phi}_b}{\sqrt{\tilde{\omega}_a^2 - \tilde{\phi}_a^2} \sqrt{\tilde{\omega}_b^2 - \tilde{\phi}_b^2}}. \quad (9)$$

Note that in the normal state $C_{ab}(\omega) = 0$ and $I(\omega) = 1$.

The dimensionless constant ζ is related to the inter-band impurity scattering rate in the normal state γ_{ab}^N as

$$\gamma_{ab}^N = \frac{n_{imp}}{\pi N_a} \zeta. \quad (10)$$

The dependence of $\gamma_{\alpha,\beta}^N$ and ζ on the scattering potential is shown in the Appendix.

3. Quasiparticle properties

3.1. DOS in superconductive state.

Interband scattering is expected to modify the gap functions and the tunneling density of states (DOS) in the superconducting state in a multiband superconductor. In the weak coupling regime the impurity effects have been discussed in [12] within the Born limit and extended in [13] to the strong coupling case. In the following we will calculate the gap functions, and the superconducting DOS by solving the nonlinear Eliashberg equations in the s_{\pm} and s_{++} superconductors for various values of the interband nonmagnetic scattering rate, going beyond the Born approximation.

Total DOS in superconducting state is given by the following expression

$$N(\omega) = \sum_{\alpha} N_{\alpha}(0) \operatorname{Re} \frac{\omega}{\sqrt{\omega^2 - \Delta_{\alpha}^2(\omega + i\delta)}}, \quad (11)$$

where we have introduced the *complex order parameter*:

$$\Delta_{\alpha}(\omega + i\delta) \equiv \omega \tilde{\phi}_{\alpha}(\omega + i\delta) / \tilde{\omega}_{\alpha}(\omega + i\delta) = \operatorname{Re} \Delta_{\alpha}(\omega) + i \operatorname{Im} \Delta_{\alpha}(\omega). \quad (12)$$

The solution for $\Delta_{\alpha}(\omega)$ allows the calculation of the current-voltage characteristic $I(V)$ and *tunnelling conductance* $G_{NS}(V) = dI_{NS}/dV$ in the superconducting state of the *NIS* tunneling junction.

In contrast to a single band case, where DOS does not depend on *nonmagnetic* impurities in the multiband case $\Delta_{\alpha}(\omega + i\delta)$ and DOS are strongly dependent on interband impurity scattering.

Figure 1 shows the calculated gap functions $\Delta_{\alpha}(\omega)$ for the bands a and b for different interband impurity scattering rates. One sees in both s_{\pm} and s_{++} cases strong non-monotonic frequency dependence of the gap function with the maximums of the absolute values around 250cm^{-1} for a -band 140cm^{-1} for b -band, originated from the strong electron-boson coupling. Furthermore, the effects of impurity scattering are visible as additional structure at low energies comparable to the interband scattering rate Γ_a . The most spectacular effect is the impurity-induced sign change of $\text{Re}\Delta(\omega)$ at low energies in b -band in the s_{\pm} state. This $s_{\pm} \rightarrow s_{++}$ transition was predicted in Matsubara representation in our earlier paper [8], where its consequences for non-vanishing T_c vs disorder behavior were discussed.

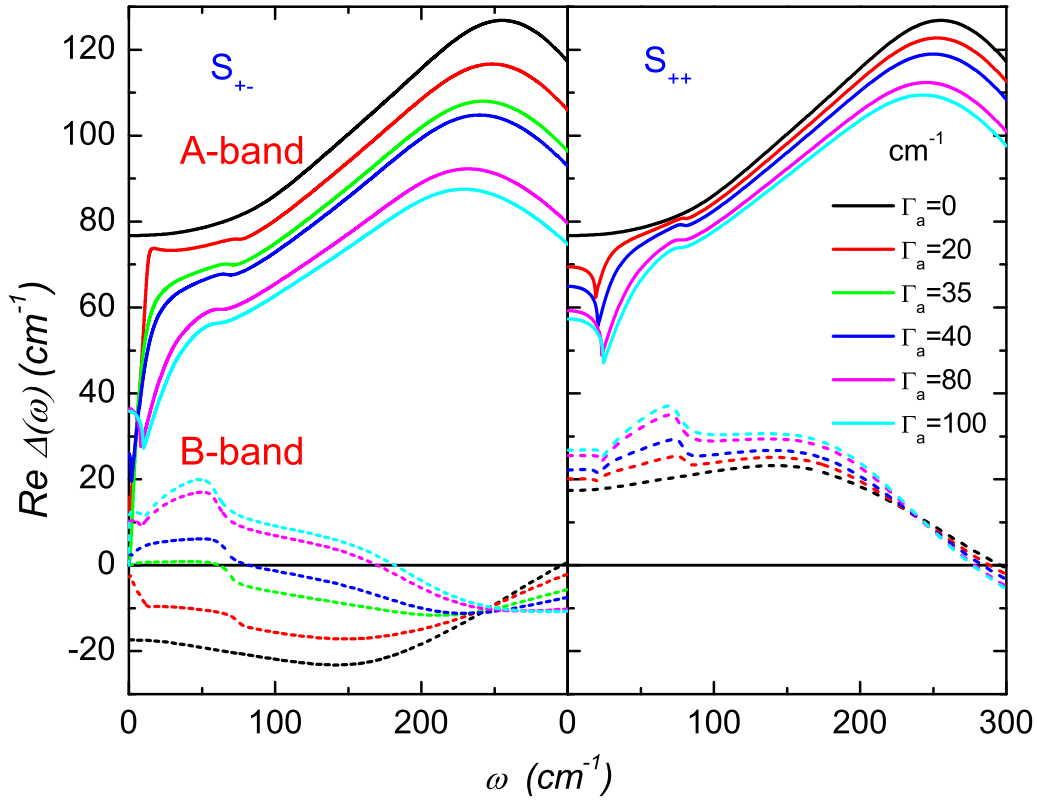


Figure 1. Superconducting gap functions for bands a and b at various interband impurity scattering rates in s_{\pm} and s_{++} models. The parameters are $\zeta \approx 0.2$, $\gamma_{bb}^N = 2\gamma_{aa}^N = \gamma_{ab} = 2\gamma_{ba}^N \approx 0.4\Gamma_a$. They corresponds to scattering strength $\sigma = 0.5$. The relation between σ and Γ_a to the scattering potential is given in the Appendix.

Figure 2 shows comparison of DOS in s_{\pm} and s_{++} states for different magnitudes

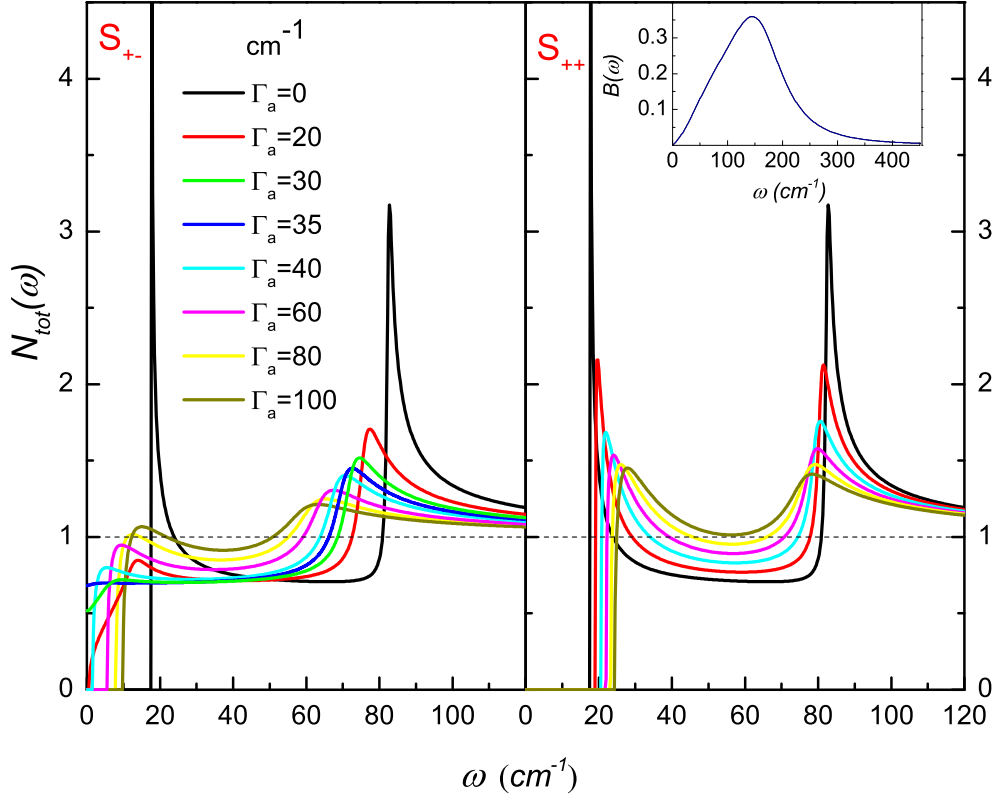


Figure 2. Total density of states for various impurity scattering rates in s_{\pm} and s_{++} models at low temperature $T \ll T_{c0}$. The parameters are the same as in Fig. 1. Inset shows the electron-boson interaction function $B(\Omega)$.

of the interband scattering rate Γ_a at low temperatures $T \ll T_{c0}$. In the clean limit, one sees two different excitations gaps for the two bands. In accordance with earlier calculations for s_{++} superconductors [13], the interband impurity scattering mixes the pairs in the two bands, so that the states appear in the a -band at the energy range of the b -band gap. These states are gradually filled in with increasing scattering rate. At the same time the minimal b -band gap in the DOS raises due to increased mixing to the a -band with strong electron-boson coupling. In the s_{\pm} superconductor, the modifications of low-energy DOS with interband impurity scattering is completely different. Due to sign change of $Re\Delta(\omega)$ in the b -band, gapless region exists in a range of values of scattering parameter Γ around 35 cm^{-1} , as clearly seen in the left panel in Fig.2. Such gapless behavior manifests itself in optical properties of s_{\pm} superconductors, as will be demonstrated below.

3.2. ARPES and the self-energy

Angle-resolved photo emission spectroscopy (ARPES) probes the photoemission current $I(\mathbf{k}, \omega)$, which can be calculated as:

$$I(\mathbf{k}, \omega) = \sum_{\alpha} |M_{\alpha}(\mathbf{k}, \omega)|^2 f(\omega) A_{\alpha}(\mathbf{k}, \omega).$$

Here $M(\mathbf{k}, \omega)$ is the dipole matrix element that depends on the initial and final electronic states, incident photon energy and polarization, $f(\omega)$ is the Fermi distribution function and

$$A_{\alpha}(\mathbf{k}, \omega) = -\frac{1}{2\pi} \text{Tr} \left\{ \text{Im} \hat{G}_{\alpha}(\mathbf{k}, \omega) \hat{\tau}_0 \right\} = -\frac{1}{\pi} \text{Im} \frac{\tilde{\omega}_{\alpha}(\omega)}{\tilde{\omega}_{\alpha}^2(\omega) - \xi_{\alpha}^2(\mathbf{k}) - \tilde{\phi}_{\alpha}^2(\omega)} \quad (13)$$

is single particle response function.

In the weak coupling limit the contribution of the electron-boson interaction to self-energy $\Sigma_{\alpha 0}(\mathbf{k}, \omega)$ (see first terms in l.h.s. of Eqs. 4, 5) vanishes. It means, that in the model with isotropic self-energy $\Sigma_{\alpha 0}^{e-b}(\omega) \rightarrow 0$, $\Sigma_{\alpha 1}^{e-b}(\omega) \rightarrow \Delta_{\alpha}(\omega)$. Then the single particle spectral function takes the form:

$$A_{\alpha}(\mathbf{k}, \omega) = \frac{1}{\pi} \text{Im} \frac{\omega \left[1 + i \sum_{\beta=a,b} \Gamma_{\alpha\beta} / \sqrt{\omega^2 - \Delta_{\beta}^2(\omega)} \right]}{D}$$

with

$$D = \xi_{\alpha}^2(\mathbf{k}) + \left(\sum_{\beta=a,b} \Gamma_{\alpha\beta} \right)^2 - \omega^2 + \Delta_{\alpha}^2(\omega) - 2i \sum_{\beta=a,b} \Gamma_{\alpha\beta} \frac{[\omega^2 + \Delta_{\alpha}(\omega)\Delta_{\beta}(\omega)]}{\sqrt{\omega^2 - \Delta_{\beta}^2(\omega)}}.$$

In the gaped regime $A_{\alpha}(\mathbf{k}, \omega)$ vanishes below Δ_{β} but in the gapless one for b -band is the same as in the normal state:

$$A_b(\mathbf{k}, \omega) = \frac{1}{\pi} \text{Im} \frac{\omega \left[1 + i \sum_{\beta=a,b} \Gamma_{b\beta} / |\omega| \right]}{\xi_b^2(\mathbf{k}) - \omega^2 \left(1 + i \sum_{\beta=a,b} \Gamma_{b\beta} / |\omega| \right)^2}.$$

The quasi-particle spectral function $A_b(\mathbf{k}, \omega)$ given by Eq.(13) for b -band is shown in Fig.3. In this case the behavior of $A_b(\mathbf{k}, \omega)$ at small ω and ξ reflects the existence of well-defined energy gap. In contrast to that, the function $A_b(\mathbf{k}, \omega)$ in the regime of $s_{\pm} \rightarrow s_{++}$ transition shows no gap, as seen from Fig.4. With further increase of scattering rate Γ_a , when s_{++} state is realized, in the b -band energy gap appears again. Therefore, ARPES measurements at various impurity concentrations may provide useful tool to distinguish underlying pairing symmetry of superconducting state in pnictides.

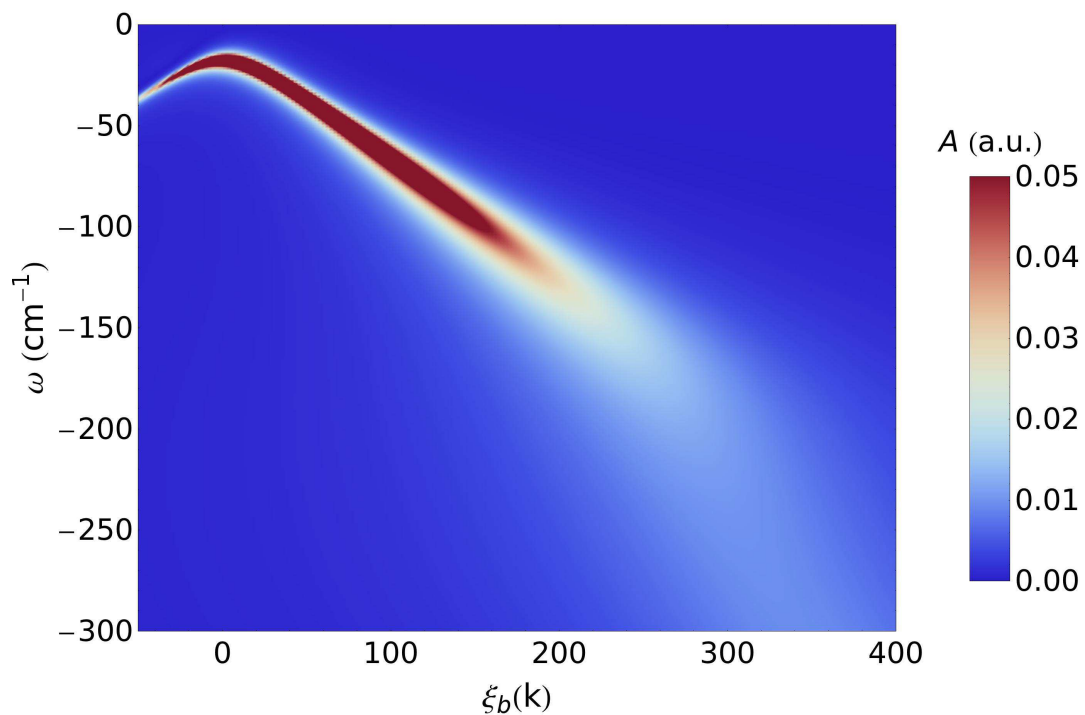


Figure 3. The quasi-particle spectral function $A_b(\mathbf{k}, \omega)$ for b -band with a small gap in the clean limit. The parameters are the same as in Fig. 1.

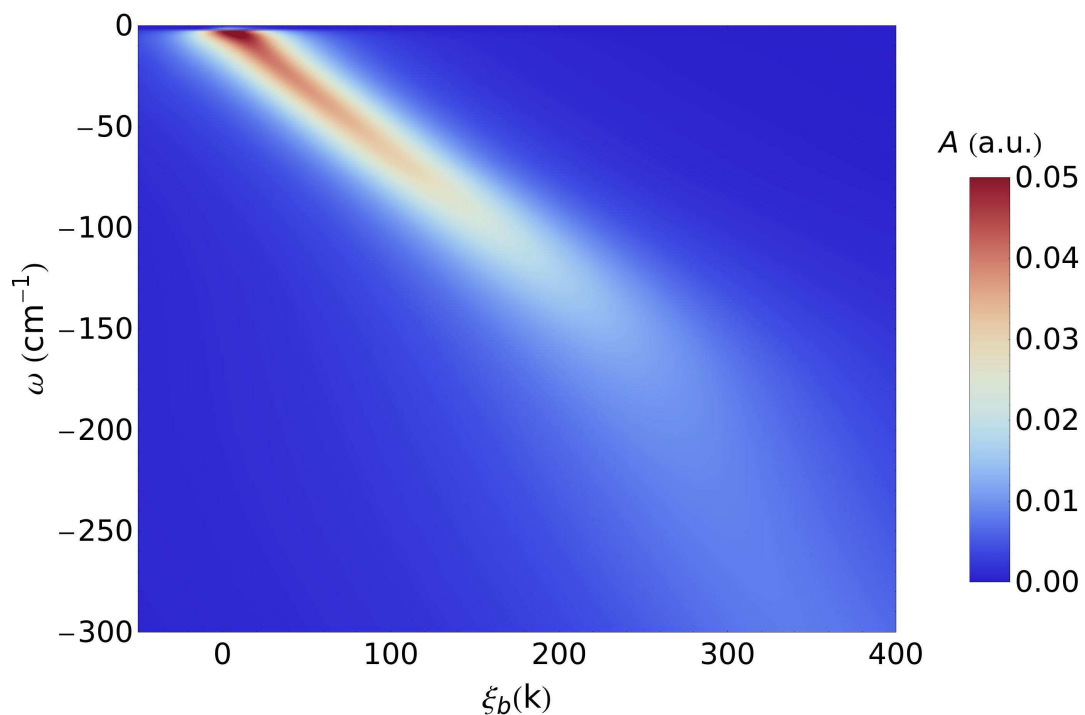


Figure 4. The quasi-particle spectral function $A_b(\mathbf{k}, \omega)$ for b -band with a small gap in the gapless regime ($\Gamma_a = 40 \text{ cm}^{-1}$). The parameters are the same as in Fig. 1.

4. Optical conductivity

The optical conductivity in the London (local, $\mathbf{q} \equiv 0$) limit in a - b plane is given by

$$\sigma(\omega) = \sum_{\alpha} \omega_{pl,\alpha}^2 \Pi_{\alpha}(\omega) / 4\pi i \omega, \quad (14)$$

where $\Pi_{\alpha}(\omega)$ is an analytical continuation to the real frequency axis of the polarization operator (see, e.g. Refs. [15],[16],[17],[18],[19])

$$\Pi_{\alpha}(\omega) = \left\{ i\pi T \sum_n \Pi_{\alpha}(\omega'_n, \nu_m) \right\}_{i\nu_m \implies \omega + i0^+},$$

$\alpha = a, b$ is the band index.

$$\begin{aligned} \Pi_{\alpha}(\omega) = \int d\omega' \left\{ \frac{\tanh\left(\frac{\omega_-}{2T}\right)}{D^R} \left[1 - \frac{\tilde{\omega}_-^R \tilde{\omega}_+^R + \tilde{\phi}_-^R \tilde{\phi}_+^R}{Q_-^R Q_+^R} \right] - \frac{\tanh\left(\frac{\omega_+}{2T}\right)}{D^A} \left[1 - \frac{\tilde{\omega}_-^A \tilde{\omega}_+^A + \tilde{\phi}_-^A \tilde{\phi}_+^A}{Q_-^A Q_+^A} \right] \right. \\ \left. - \frac{\tanh\left(\frac{\omega_+}{2T}\right) - \tanh\left(\frac{\omega_-}{2T}\right)}{D^a} \left[1 - \frac{\tilde{\omega}_-^A \tilde{\omega}_+^R + \tilde{\phi}_-^A \tilde{\phi}_+^R}{Q_-^A Q_+^R} \right] \right\}, \quad (15) \end{aligned}$$

where

$$\begin{aligned} Q_{\pm}^{R,A} &= \sqrt{(\tilde{\omega}_{\pm}^{R,A})^2 - (\tilde{\phi}_{\pm}^{R,A})^2}, \\ D^{R,A} &= \sqrt{(\tilde{\omega}_+^{R,A})^2 - (\tilde{\phi}_+^{R,A})^2} + \sqrt{(\tilde{\omega}_-^{R,A})^2 - (\tilde{\phi}_-^{R,A})^2}, \end{aligned}$$

and

$$D^a = \sqrt{(\tilde{\omega}_+^R)^2 - (\tilde{\phi}_+^R)^2} - \sqrt{(\tilde{\omega}_-^A)^2 - (\tilde{\phi}_-^A)^2},$$

$\omega_{\pm} = \omega' \pm \omega/2$, and the index $R(A)$ corresponds to the retarded (advanced) brunch of the complex function $F^{R(A)} = ReF \pm iImF$ (the band index α is omitted).

In the normal state the conductivity is

$$\sigma_{\alpha}^N(\omega) = \frac{\omega_{pl}^2}{8i\pi\omega} \int_{-\infty}^{\infty} dz \frac{\tanh((z+\omega)/2T) - \tanh(z/2T)}{\tilde{\omega}_{\alpha}(z+\omega) - \tilde{\omega}_{\alpha}(z)}.$$

If the dominant contribution to the quasiparticle damping comes from the impurity scattering, it reduces to the Drude formula:

$$\sigma_a(\omega, T) = \frac{\omega_{pl}^2}{4\pi} \frac{1}{\gamma_a^{opt} - i\omega}$$

with $\gamma_a^{opt} = \gamma_{ab} + \gamma_{aa}$.

In the Fig. 5 we demonstrate the impact of disorder on the optical conductivity $Re\sigma(\omega)$. In the clean limit one sees $Re\sigma_{\alpha}(\omega) = 0$ for $\omega < 2\Delta_{\alpha}$. With increase the impurity scattering rate the region $Re\sigma_b(\omega) = 0$ for the band b decreases and the peak above $2\Delta_b$ becomes sharper. It is clearly seen that in the vicinity of transition from the s_{\pm} to s_{++} state ($\Gamma_a \sim 35cm^{-1}$), the conventional Drude-response characteristic

in the weak for a normal metal-state is realized. The origin of this effect is gapless nature of superconductivity near the impurity-induced $s_{\pm} \rightarrow s_{++}$ transition. With further increase of the impurity scattering rate, the optical conductivity recovers gapped-like behavior, but with smaller gap. It is strikingly different from the behavior of superconductors with s_{++} order parameter (Fig. 5.b), where values of two gaps tends to merge at the limit of infinite impurity scattering rate. This reentrant behavior of optical conductivity with concentration of nonmagnetic impurities may serve as unambiguous indication for the s_{\pm} order parameter symmetry.

Another important characteristic of the superconducting state is the real part of the electromagnetic kernel (polarization operator) which is related to the imaginary part of optical conductivity $Im\sigma(\omega)$ (see Eq.14). Fig.6 shows the frequency dependence of $Re\Pi(\omega)$ for s_{\pm} and s_{++} models for various interband scattering rates. One can see that in the s_{++} case dips at $\omega = 2\Delta_{\alpha}(\omega)$ occur for nonzero scattering, in accordance with previous calculations done for single-band superconductors [20]. Further, an interesting peculiarity is seen in the response of the b -band in the s_{\pm} state: the dip position is a nonmonotonic function of interband scattering rate and the dip vanishes completely in the gapless regime corresponding to the $s_{\pm} \rightarrow s_{++}$ transition.

Magnetic field penetration depth $\lambda_L(T)$ in the local (London) limit in a - b plane is related to $Im\sigma(\omega)$ in zero frequency limit

$$1/\lambda_L^2(T) = \sum_{\alpha=a,b} \lim_{\omega \rightarrow 0} 4\pi\omega \text{Im} \sigma_{\alpha}(\omega, \mathbf{q} = 0, T)/c^2, \quad (16)$$

where c is the velocity of light. If we neglect strong-coupling effects (or, more generally, Fermi-liquid effects) then for a clean uniform superconductor at $T = 0$ we have the relation $\lambda_L = c/\omega_{pl}$, where $\omega_{pl,\alpha} = \sqrt{8\pi e^2 \langle N_{\alpha}(0) v_{F\alpha} v_{F\alpha} \rangle}$ is the plasma frequency in different bands.

Partial contributions to the magnetic field penetration depth can be written as

$$1/\lambda_L^2(T) = Re \sum_{\alpha=a,b} \frac{\omega_{pl,\alpha}^2}{c^2} \int_{\omega_g(T)-0}^{\infty} \frac{d\omega \tanh(\omega/2T)}{Z_{\alpha}(\omega, T) \sqrt{\omega^2 - \Delta_{\alpha}^2(\omega, T)} [\Delta_{\alpha}^2(\omega, T) - \omega^2]}. \quad (17)$$

Here the points $\omega_g(T)$ are determined by the condition for the density of states in the band

$$ReN(\omega < \omega_g(T)) = 0.$$

For superconductors with gap nodes as well as for $T > 0$: $\omega_g(T) \equiv 0$ (see, [21]).

Peculiarities of the penetration depth in the crossover regime from s_{\pm} to s_{++} state have been discussed earlier [8].

5. Conclusions

We have studied the effects of the impurity-induced $s_{\pm} \rightarrow s_{++}$ transition in the density of states, the single particle response function and optical conductivity in a multiband superconductors with s_{\pm} symmetry of the order parameter. It has been shown that smaller gap vanishes in the vicinity of this transition, leading to gapless nature of

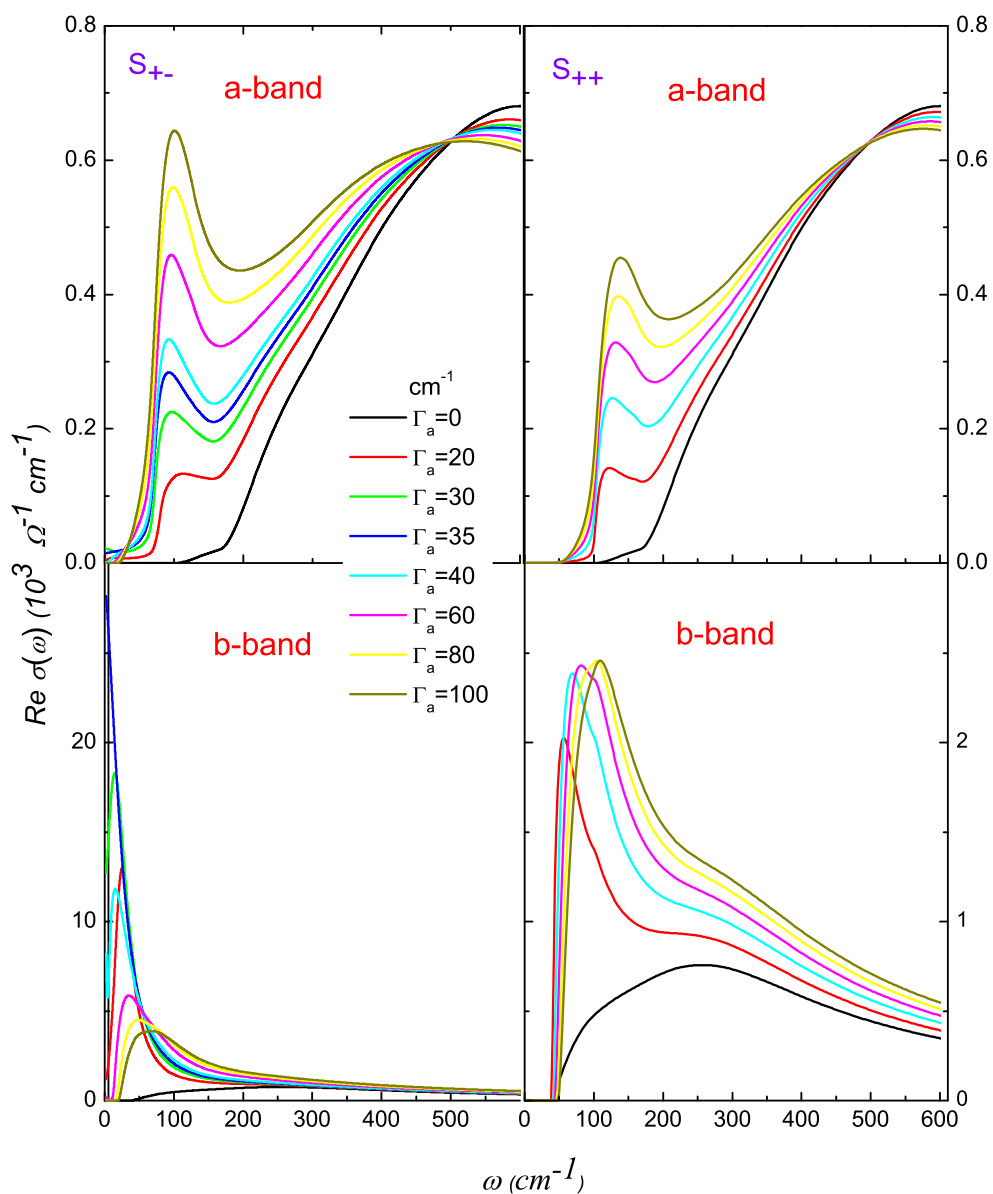


Figure 5. Real part of the optical conductivity $Re\sigma(\omega)$ for various values of Γ_a . The parameters are the same as in Fig. 1.

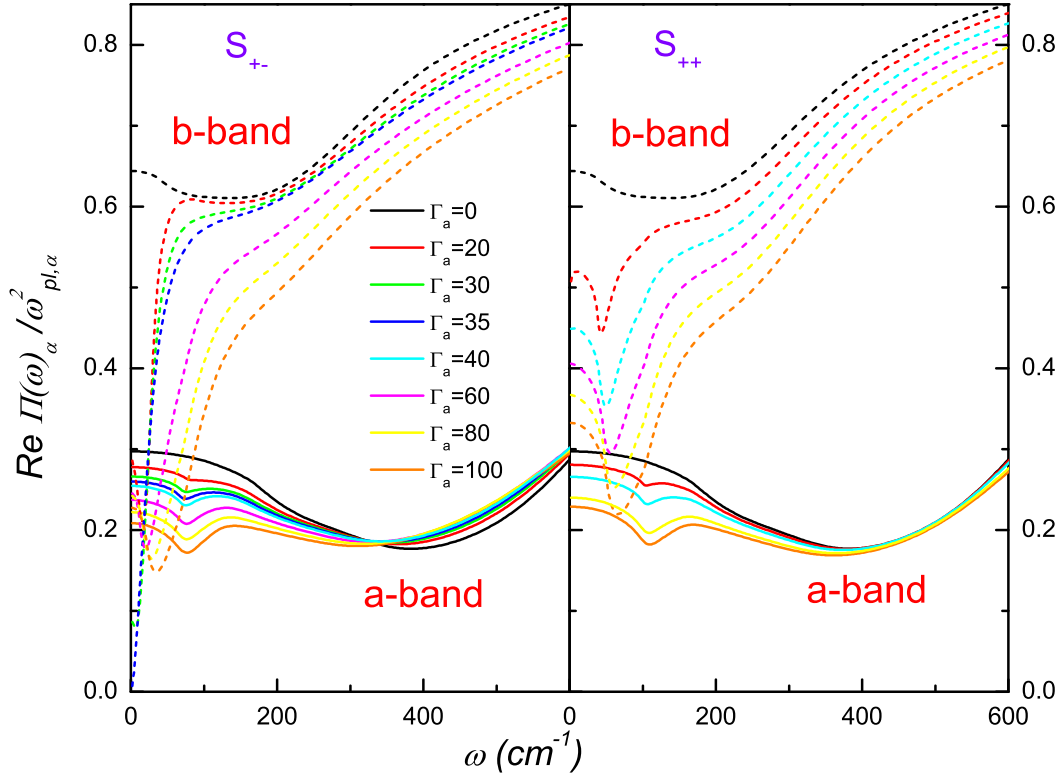


Figure 6. Real part of the polarization operator for various values of Γ_a . The parameters are the same as in Fig. 1.

photoemission and tunneling spectra. In optical response, the $s_{\pm} \rightarrow s_{++}$ transition leads to "restoring" of the "Drude"-like frequency dependence of $Re\sigma(\omega)$. We have also found interesting anomalies in the real part of polarization operator, with reentrance behavior of the dip-like structure at $\omega = 2\Delta_{\alpha}(\omega)$ as a function of interband scattering rate. This effect leads to non-monotonic behavior in the magnetic field penetration depth as a function of the impurity concentration.

We want to stress that systematic study of the impact of disorder on the single-particle response function and optical conductivity may give an information about underlying symmetry of the superconductive order parameter.

Acknowledgments

The authors are grateful to P. Hirschfeld, M.M. Korshunov, A. Charnukha, A.V. Boris, B. Keimer for useful discussions. The present work was partially supported by the DFG Priority Programme SPP1458 (DVE), Dutch FOM (AAG).

Appendix

The impurity part of the self energy is obtained by analytic continuation of the correspondent self-energy on Matsubara frequencies $\hat{\Sigma}_{\alpha\beta}^{imp}(i\omega_n) = \Sigma_{\alpha\beta}^{imp(0)}(i\omega_n)\hat{\tau}_0 + \Sigma_{\alpha\beta}^{imp(3)}(i\omega_n)\hat{\tau}_3$ derived in [8]. The last is taken in the T - matrix approximation:

$$\hat{\Sigma}^{imp}(\omega_n) = n_{imp}\hat{\mathbf{U}} + \hat{\mathbf{U}}\hat{\mathbf{g}}(\omega_n)\hat{\Sigma}^{imp}(i\omega_n), \quad (\text{A.1})$$

where $\hat{\mathbf{U}} = \mathbf{U} \otimes \hat{\tau}_3$ and n_{imp} is the impurity concentration and the scattering potential:

$$\mathbf{U} = \begin{pmatrix} U_{aa} & U_{ba} \\ U_{ab} & U_{bb} \end{pmatrix}.$$

The quasiclassical Nambu Green's functions on Matsubara frequencies are:

$$g_{0\alpha} = -\frac{i\pi N_{\alpha}\tilde{\omega}_{\alpha n}}{\sqrt{\tilde{\omega}_{\alpha n}^2 + \tilde{\phi}_{\alpha n}^2}}, \quad g_{1\alpha} = -\frac{\pi N_{\alpha}\tilde{\phi}_{\alpha n}}{\sqrt{\tilde{\omega}_{\alpha n}^2 + \tilde{\phi}_{\alpha n}^2}}. \quad (\text{A.2})$$

Solutions of Eqs. (A.1) for $\Sigma_{aa}^{imp(0)}$ and $\Sigma_{aa}^{imp(1)}$ are

$$\Sigma_{aa}^{imp(0)} = n_{imp} \frac{U_{aa}^2 - (\det \mathbf{U})^2 (g_{0b}^2 - g_{1b}^2)}{D(\omega_n)} g_{0b} + n_{imp} \frac{U_{ab}U_{ba}}{D(\omega_n)} g_{0b}, \quad (\text{A.3})$$

$$\Sigma_{aa}^{imp(1)} = -n_{imp} \frac{U_{aa}^2 - (\det \mathbf{U})^2 (g_{0b}^2 - g_{1b}^2)}{D(\omega_n)} g_{1a} - n_{imp} \frac{U_{ab}U_{ba}}{D(\omega_n)} g_{1b}, \quad (\text{A.4})$$

where

$$D(\omega_n) = 1 - (g_{0a}^2 - g_{1a}^2) U_{aa}^2 - (g_{0b}^2 - g_{1b}^2) U_{bb}^2 + (g_{0a}^2 - g_{1a}^2) (g_{0b}^2 - g_{1b}^2) (\det \mathbf{U})^2 - 2U_{ab}U_{ba} (g_{0a}g_{0b} - g_{1a}g_{1b}). \quad (\text{A.5})$$

The analytical continuation on the real axis leads to the following expression:

$$\hat{\Sigma}^{imp(0)}(\omega) = \sum_{\beta=a,b} i\Gamma_{\alpha\beta}(\omega) \frac{\tilde{\omega}_{\beta}(\omega)}{\sqrt{\tilde{\omega}_{\beta}^2(\omega) - \tilde{\phi}_{\beta}^2(\omega)}},$$

and

$$\hat{\Sigma}^{imp(1)}(\omega) = \sum_{\beta=a,b} i\Gamma_{\alpha\beta}(\omega) \frac{\tilde{\phi}_{\beta}(\omega)}{\sqrt{\tilde{\omega}_{\beta}^2(\omega) - \tilde{\phi}_{\beta}^2(\omega)}}$$

with $\Gamma_{\alpha\beta}(\omega)$ given by Eq.(7).

The dimensionless constant ζ is convenient to express in terms of dimensionless scattering potentials $\bar{u}_{\alpha\beta} = \pi U_{\alpha\beta} N_{\beta}$ and $\bar{d} = \bar{u}_{aa}\bar{u}_{bb} - \bar{u}_{ab}\bar{u}_{ba}$. Then it has the following compact form:

$$\zeta = \frac{\bar{u}_{ab}\bar{u}_{ba}}{(\bar{d} - 1)^2 + (\bar{u}_{aa} + \bar{u}_{bb})^2}. \quad (\text{A.6})$$

Normal state impurity scattering rate reads:

$$\gamma_{\alpha\alpha}^N = \frac{n_{imp}}{\pi N_{\alpha}} \frac{\bar{d}^2 + \bar{u}_{\alpha\alpha}^2}{(\bar{d} - 1)^2 + (\bar{u}_{aa} + \bar{u}_{bb})^2} \quad (\text{A.7})$$

and for $\alpha \neq \beta$

$$\gamma_{\alpha\beta}^N = \frac{n_{imp}}{\pi N_{\alpha}} \frac{\bar{u}_{ab}\bar{u}_{ba}}{(\bar{d} - 1)^2 + (\bar{u}_{aa} + \bar{u}_{bb})^2}. \quad (\text{A.8})$$

The Born approximation corresponds to $\bar{u}_{\alpha\beta} \ll 1$. Then up to quadratic terms in \bar{u} one gets:

$$\Gamma_{aa}(\omega) \approx \gamma_{aa}^N \approx n_{imp}\pi N_a U_{aa}^2$$

and

$$\Gamma_{ab}(\omega) \approx \gamma_{ab}^N \approx n_{imp}\pi N_b U_{ab}^2.$$

It is worth to introduce the parameters $\sigma = \bar{u}_{ab}\bar{u}_{ba}/(1 + \bar{u}_{ab}\bar{u}_{ba})$ and $\Gamma_a = n_{imp}\frac{\sigma}{\pi N_a} = n_{imp}\pi N_b U_{ab} U_{ba} (1 - \sigma)$. The parameter σ is used as an indicator of the strength of the impurity scattering. In the Born approximation $\sigma \rightarrow 0$, while in the opposite unitary limit $\sigma \rightarrow 1$.

References

- [1] Kamihara Y *et al.* 2008 *J. Am. Chem. Soc.* **130** 3296
- [2] See, e.g. "Superconductivity in Iron-Pnictides" in 2008 *Physica C Issues 9-12* **469**; Hirschfeld P J, Korshunov M M and Mazin I I 2011 *Rep. Prog. Phys.* **74** 124508; Kordyuk A A 2012 *Fiz. Nizk. Temp.* **38**, 1119
- [3] Evtushinsky D V *et al.* 2012 *Preprint* arXiv:1204.2432v1, Huang Y-B, Richard P, Wang X-P, Qian T and Ding H 2012 *Preprint* arXiv:1208.4717
- [4] Popovich P *et al.* 2010 *Phys. Rev. Lett.* **105** 027003
- [5] Hardy F, Burger P, Wolf T, Fisher R A, Schweiss P, Adelman P, Heid R, Fromknecht R, Eder R, Ernst D, Lohneysen H v and Meingast C 2010 *EPL* **91** 47008
- [6] Charnukha A *et al.* 2011, *Phys. Rev. B* **84**, 174511
- [7] Kontani H and Onari S 2010 *Phys. Rev. Lett.* **104** 157001 ; Senga Y and Kontani H 2008 *J. Phys. Soc. Jpn.* **77** 113710; Onari S and Kontani H 2009 *Phys. Rev. Lett.* **103** 177001
- [8] Efremov D V, Korshunov M M, Dolgov O V, Golubov A A and Hirschfeld P J 2011 *Phys.Rev.B* **84**(R) 180512
- [9] Golubov A A and Mazin I I 1997 *Phys. Rev. B* **55** 15146
- [10] Golubov A A and Mazin I I 1995 *Physica C* **243** 153
- [11] Allen P B and Mitrović B 1982 *Solid State Physics* **37** 1
- [12] Schopohl N and Scharnberg K 1977 *Solid State Commun.* **22** 371
- [13] Dolgov O V, Kremer R K, Kortus J, Golubov A A and Shulga S V 2005 *Phys. Rev. B* **72** 024504
- [14] Golubov A A, Brinkman A, Dolgov O V, Kortus J and Jepsen O 2002 *Phys. Rev. B* **66** 054524; Kogan V G, Martin C and Prozorov R 2009 *Phys. Rev. B* **80** 014507
- [15] Nam S B 1967 *Phys. Rev.* **156** 470
- [16] Lee W, Rainer D and Zimmermann W 1988 *Physica C* **159** 535
- [17] Dolgov O V, Golubov A A and Shulga S V 1990 *Phys. Letters A* **147** 317.
- [18] Akis R and Carbotte J P 1991 *Solid State Comm.* **79** 577
- [19] Marsiglio F 1991 *Phys. Rev. B* **44** 5373
- [20] Marsiglio F, Carbotte J P, Puchkov A and Timusk T 1996 *Phys. Rev. B* **53** 9433
- [21] E.G. Maksimov and D.I. Khomskii 1982 *High Temperature Superconductivity* ed V L Ginzburg and D Kirzhnits (New York: Consultant Bureau)